結晶化条件の溶媒に対して溶解度が低いため、DMSO 等の有機溶媒共存下での操作となった。

種々の条件で実験を進めたが、今年度は特に、我々が開発を進めている新しい試料マウント方法(HAG法)を適用した解析を試みた。この方法は、結晶試料を水溶性高分子の水溶液で覆い、湿度を調整したうえで、室温あるいはクライオ条件でX線回折測定を行う。グリセロール等の抗凍結剤を全く使わないあるいは量を減らして、クライオ実験を行うことを可能とする特徴がある。

Ras蛋白質結晶は、この方法によってもクライオ実験に支障はなく、良好な回折データが取得できた。薬剤の結合は確認できなかったものの、ある湿度条件においては結晶格子の転移が起こり、従来とは異なる種類の分子構造が得られることが明らかとなった。

得られた構造は、state 1に該当するがGly60主鎖とγ-リン酸の結合が残った中間体構造($GTP_{1w/HB}$)であった。これは、過去に神戸大グループとの研究協力により得られた構造（PDB ID: 3KKM）に類似しているが、Switch I/II領域の構造は全く異なっている。また、この転移は、湿度の変化によって可逆的であることも示唆され、外場による構造変化誘導の例として興味深い結果を与えている。構造の詳細は現在検討中である。

D．考察

通常、蛋白質の結晶は水溶液中で析出することもあり、25-75%の水溶媒を含んでいる。試料雰囲気の湿度制御により、この水で満たされた空間の体積を変化させることができるうえ、結晶性の改善がみられる事例も報告されている。

また、従来のクライオ実験で用いられる抗凍結剤は、比較的高濃度で使用する必要がある。たとえば、よく使われるグリセロールは分子サイズが小さいために浸透性が高く、弱いながらも蛋白質と相互作用するほか、水和分子をかく乱する恐れもあり、しばしば他の結合分子を排除する事例が見られる。

そこで、湿度調節と浸透性の抗凍結剤の排除の効果が期待できるHAG法のRas構造解析への適用を試みた。その結果、これまでに本法を適用した試料には見られない大きな格子変化が見られた。解析の結果から、分子表面のループ構造が大きく変化することで、脱水による分子の充填様式の変化を受容できたものと考えられる。このことは、Ras蛋白質が本質的にもつ柔軟さと深く関係しているものと考えられる。さらに外場環境の調整により、この柔軟性のバリエーションを網羅することができれば、柔軟さゆえに一般的には捉えられない構造を適当な格子の中に収め、さまざまに静止像を解析することが可能になる。これによって、スナップショットながら、分子の動的構造に迫ることができると考えられる。

また、本課題で目指しているRasの構造をstate 1に維持する薬剤の探索において、今回新たに得られた構造は所望の構造と言える。一般に、結晶中の分子充填に関わる分子間相互作用は強く、薬剤等の分子結合に誘導適合を必要とする場合、薬剤の親和性が低い場合にはエネルギーバリアとなりうる。それを外場による構造変化誘導により、所望の構造に変化させられれば、薬剤結合の可能性は大きく広がると言える。

E．結論

HAG法による薬剤候補化合物との複合体結晶解析に必要な手法の確立を進めた結果、本法は結晶内の分子構造を制御する可能性があることが示唆された。

柔軟な構造を持つH-Rasについては、こうした外場制御によって格子の状態を変化させることで、さまざまな分子構造を解析する可能性がある。

今後はこの構造について薬剤を浸漬させた結晶の構造決定を行う予定である。また、他の結晶系に対しても本法を適用し、Ras分子のさまざまな構造様態を解明したい。

G．研究発表

１．論文発表

Muraoka S, Shima F, Araki M, Inoue T, Yoshimoto A, Ijiri Y, Seki N, Tamura A, Kumasaka T, Yamamoto M, Kataoka T.
Crystal structures of the state 1 conformations of the GTP-bound H-Ras protein and its oncogenic G12V and Q61L mutants.
FEBS Lett. **586**:1715-1718 (2012)

２．学会発表

（本件に関してはありません。）

H．知的財産権の出願・登録状況

１．特許取得

なし

２．実用新案登録

なし

３．その他

特にありません。

Ⅲ．研究成果の刊行に関する一覧表

研究成果の刊行に関する一覧表レイアウト

書籍

著者氏名	論文タイトル名	書籍全体の編集者名	書　籍　名	出版社名	出版地	出版年	ページ

雑誌

発表者氏名	論文タイトル名	発表誌名	巻号	ページ	出版年
Shin Muraoka,Fumi Shima,Mitsugu Araki,Tomoko Inoue,Akiko Yoshimoto,Yuichi Ijiri,Nobuaki Seki,Atsuo Tamura,Takashi Kumasaka,Masaki Yamamoto,Tohru kataoka	Crystal structures of the state 1 conformations of the GTP-bound H-Ras protein and its oncogenic G12V and Q61L mutants	FEBS Letters	586	1715-1718	2012

Ⅳ. 研究成果の刊行物・別刷

FEBS Letters 586 (2012) 1715–1718

FEBS Letters

journal homepage: www.FEBSLetters.org

Crystal structures of the state 1 conformations of the GTP-bound H-Ras protein and its oncogenic G12V and Q61L mutants

Shin Muraoka [a,1], Fumi Shima [a,1], Mitsugu Araki [b], Tomoko Inoue [a], Akiko Yoshimoto [a], Yuichi Ijiri [a], Nobuaki Seki [b], Atsuo Tamura [b], Takashi Kumasaka [c], Masaki Yamamoto [d], Tohru Kataoka [a,*]

[a] Division of Molecular Biology, Department of Biochemistry and Molecular Biology, Kobe University Graduate School of Medicine, 7-5-1 Kusunoki-cho, Chuo-ku, Kobe 650-0017, Japan
[b] Department of Chemistry, Kobe University Graduate School of Science, 1-1 Rokkodai, Nada-ku, Kobe 657-8501, Japan
[c] Japan Synchrotron Radiation Research Institute (JASRI), 1-1-1 Kouto, Sayo-cho, Sayo-gun, Hyogo 679-5198, Japan
[d] RIKEN SPring-8 Center, 1-1-1 Kouto, Sayo-cho, Sayo-gun, Hyogo 679-5148, Japan

ARTICLE INFO

Article history:
Received 2 April 2012
Revised 25 April 2012
Accepted 30 April 2012
Available online 11 May 2012

Edited by Christian Griesinger

Keywords:
Ras
Small GTPases
Oncogene
Crystal structure
Conformational dynamics

ABSTRACT

GTP-bound Ras adopts two interconverting conformations, "inactive" state 1 and "active" state 2. However, the tertiary structure of wild-type (WT) state 1 remains unsolved. Here we solve the state 1 crystal structures of H-Ras WT together with its oncogenic G12V and Q61L mutants. They assume open structures characterized by impaired interactions of both Thr-35 in switch I and Gly-60 in switch II with the γ-phosphate of GTP and possess two surface pockets of mutually different shapes unseen in state 2, a potential target for selective inhibitor development. Furthermore, they provide a structural basis for the low GTPase activity of state 1.

1. Introduction

Small GTPases H-Ras, K-Ras, and N-Ras, the products of the *ras* proto-oncogenes, function as molecular switches by cycling between GTP-bound active and GDP-bound inactive forms in intracellular signaling pathways controlling cell growth, differentiation, and apoptosis [1]. Their interconversion is reciprocally catalyzed by guanine nucleotide exchange factors and GTPase-activating proteins (GAPs) [1]. In particular, GAPs enhance the intrinsic GTPase activity of Ras, leading to its inactivation. The oncogenic potential of Ras is activated by point mutations mainly at codons 12 and 61, the most prevalent of which in human cancers are those yielding G12V and Q61L substitutions. Most of these mutations impair the intrinsic GTPase activity and moreover render Ras insensitive to the GAP action, leading to constitutive activation of downstream effectors such as Raf kinases and phosphoinositide 3-kinases [1,2]. Crystal structures of H-Ras revealed that the exchange of GDP for GTP causes allosteric conformational changes in two adjacent regions, switch I (residues 32–38) and switch II (residues 60–75) [2]. Switch I almost overlaps with the effector region (residues 32–40), which forms a principal interface for effector recognition [2]. Besides, ^{31}P NMR studies revealed that H-Ras in complex with GTP or its non-hydrolyzable analog such as guanosine 5′-[β,γ-imido]triphosphate (GppNHp) exhibits dynamic equilibrium between two interconverting conformations, called state 1 and state 2, which are characterized by different chemical shift values for the resonances of the γ- and α-phosphate groups of GTP [3]. Because association with the various effectors, such as c-Raf-1, shifted the equilibrium toward state 2, state 1 and state 2 are regarded as "inactive" and "active" conformations, respectively [3]. Although crystal structures corresponding to state 2 were solved with wild-type (WT) H-Ras alone or in complex with the effectors [4,5], those corresponding to state 1 have only been solved with its mutants carrying T35S, G60A, and Y32F substitution [6–8] and M-RasWT [9], but not with H-Ras WT. It was revealed that state 1 assumes an open structure distinguishable from state 2 by the loss of the direct and Mg^{2+}-coordinated indirect hydrogen-bonding interactions of Thr-35 in switch I with the γ-phosphate of GppNHp, which causes marked deviation away from the guanine nucleotide and conformational instability of the switch I loop [6]. Further analyses showed the importance of the Gly-60-γ-phosphate direct hydrogen-bonding interaction and

Abbreviations: GAP, GTPase-activating protein; GppNHp, guanosine 5′-(β,γ-imido)triphosphate; RBD, Ras-binding domain; WT, Wild type; rms, root mean square

* Corresponding author. Fax: +81 78 382 5399.
E-mail address: kataoka@people.kobe-u.ac.jp (T. Kataoka).
[1] These authors contributed equally to this work.

0014-5793/$36.00 © 2012 Federation of European Biochemical Societies. Published by Elsevier B.V. All rights reserved.
http://dx.doi.org/10.1016/j.febslet.2012.04.058

the switch II-α3-helix interaction in stabilizing the state 2 conformation [6,10]. In particular, H-RasT35S-GppNHp yielded two distinct state 1 crystal structures, form 1 and form 2, showing the existence of polysterism in switch I and switch II [6]. The solution structure of H-RasT35S-GppNHp also revealed polysterism in the switch regions, prominent in switch I [11].

In the present study, we succeed in solving the state 1 crystal structures of H-RasWT, G12V, and Q61L in complex with GppNHp for the first time. Comparison with the WT state 2 structure provides a structural basis for the lower GTPase activity of state 1.

2. Materials and methods

2.1. Protein purification

Residues 1–166 of human H-RasWT, G12V, T35S, and Q61L, and the Ras-binding domain (RBD, residues 50–131) of human c-Raf-1 were expressed as fusions with glutathione S-transferase in *Escherichia coli* using pGEX-6P-1 vector (GE Healthcare), immobilized on glutathione-agarose resin, and eluted by cleavage with PreScission protease (GE Healthcare). H-Ras polypeptides were loaded with GppNHp after further purification by ion exchange chromatography.

2.2. NMR spectroscopy

^{31}P NMR spectra were recorded in the presence or absence of c-Raf-1 RBD on Brucker AVANCE-500 NMR spectrometer [9] and referenced as described before [12].

2.3. Cross-seeding method for crystallization of H-Ras-GppNHp state 1

Crystals of H-RasWT, G12V, and Q61L in complex with Mg^{2+} and GppNHp (16, 6, and 6 mg/ml, respectively) were grown on seeds of a few pieces of finely pulverized crystals of H-RasT35S-GppNHp form 1 [6], which were transferred by using Disposable Crystal Probe manipulators (Hampton Research), at 20 °C by the sitting drop vapor diffusion method using a reservoir solution containing 100 mM 2-(*N*-morpholino)ethanesulfonic acid, pH 6.5, 200 mM ammonium sulfate, and 30% (w/v) PEG5000 MME. In addition, 1,5-diaminopentane dihydrochloride and β-nicotinamide adenine dinucleotide hydrate were added to the droplets of H-RasWT and Q61L, respectively. A MALDI-TOF mass spectroscopy confirmed that the H-RasWT-GppNHp crystals almost exclusively consisted of the WT protein.

2.4. Data collection and structure determination

The data collections at 100 K were carried out at the BL41XU beamline using MX225HE (Rayonix) CCD detector in SPring-8. The data were processed using the program MOSFLM [13] and scaled with SCALA in the CCP4 program suite [14]. For crystallographic refinement, the crystal structure of H-RasT35S-GppNHp form 1 was used as an initial model for H-RasWT-GppNHp, which was subsequently used for refining the crystal structures of H-RasG12V-GppNHp and H-RasQ61L-GppNHp. The crystal structures of H-RasWT, G12V, and Q61L were refined at 1.90 Å, 1.90 Å, and 2.30 Å resolutions, respectively, with the program REFMAC [15]. After each refinement calculation, the obtained models were corrected with a $2F_o - F_c$ map using COOT [16]. The data collection and refinement statistics are summarized in Supplemental Table I.

2.5. Graphics

Figures were prepared with the programs Raster3D [17] and MOLSCRIPT [18].

2.6. Protein Data Bank (PDB) codes of the coordinates used in this study

H-RasWT-GppNHp (state 1), 4EFL; H-RasG12V-GppNHp (state 1), 4EFM; H-RasQ61L-GppNHp (state 1), 4EFN; H-RasWT-GppNHp (state 2), 5P21; H-RasY32F-GppNHp, 3K9N; H-RasT35S-GppNHp form 1, 3KKN; H-RasT35S-GppNHp form 2, 3KKM; H-RasG60A-GppNHp, 1XCM.

3. Results and discussion

3.1. Crystal structures of H-RasWT, G12V, and Q61L correspond to state 1

The state 1 population occupies 36 ± 2% and 53% for H-RasWT-GppNHp and H-RasG12V-GppNHp, respectively [6,19]. H-RasQ61L-GppNHp also exhibited a comparable state 1 population of 58 ± 2% as shown by ^{31}P NMR (Supplemental Fig. 1). Our multidimensional heteronuclear NMR analysis of H-RasWT-GppNHp had shown that the backbone resonance signals for multiple residues were split into two peaks, one of which coincided well with those of H-RasT35S-GppNHp exclusively adopting state 1 [11]. This prompted us to grow H-RasWT state 1 crystals on the seeds of H-RasT35S-GppNHp crystals. By using the H-RasT35S-GppNHp form 1 crystals with the *I*222 space group as seeds, we obtained crystals of H-RasWT-GppNHp with the same space group. Moreover, subsequent trials for H-RasG12V and Q61L mutants successfully yielded similar crystals. Final $2F_o - F_c$ electron density maps obtained by a crystallographic refinement were clear for all the 166 residues and GppNHp (Supplemental Fig. 2) of WT, G12V, and Q61L with the resolution of 1.90 Å, 1.90 Å, and 2.30 Å, respectively. The structures adopted a Rossmann fold composed of 5 α-helices and 6 β-strands (Fig. 1). Least square fitting showed that the backbone structures of G12V and Q61L, including switch I and switch II, were superimposed very well on that of WT with root-mean-square (rms) deviations of 0.06 and 0.10 Å for 166 Cα atoms, respectively. The backbone structures of the P-loop (residues 10–17) and switch II

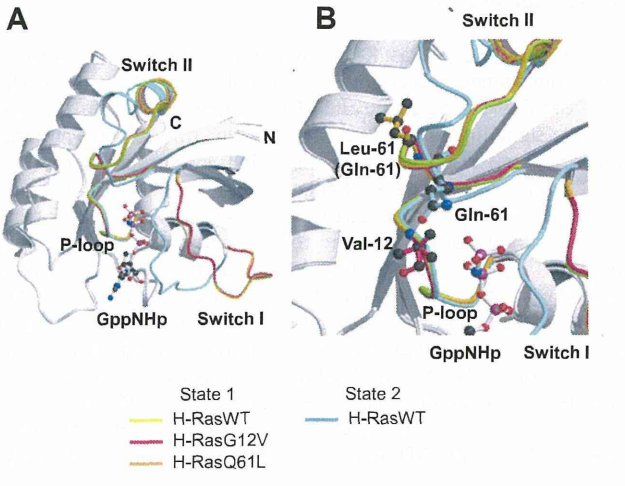

Fig. 1. Comparison of the crystal structures among H-RasWT-GppNHp and its mutants. Superimposition of the backbone structures of the P-loop, switch I, and switch II among WT state 1 (4EFL, *green*), G12V state 1 (4EFM, *deep pink*), Q61L state 1 (4EFN, *orange*), and WT state 2 (5P21, *cyan*) shown in the *ribbon model*. The other regions are overlapped very well and shown in *gray*. GppNHp of WT state 1 is shown in the *ball-and-stick model* (*red*, oxygen; *blue*, nitrogen; *deep pink*, phosphorus). (B) An enlargement of the structures surrounding Val-12 in G12V state 1 (4EFM, *deep pink*), Leu-61 in Q61L state 1 (4EFN, *orange*), and Gln-61 in WT state 2 (5P21, *cyan*), which are highlighted by the *ball-and-stick model*.

appeared unaffected by the G12V and Q61L substitutions, respectively. On the other hand, the backbone structures of their switch regions exhibited a marked deviation from that of H-RasWT state 2 (Fig. 1). Particularly, residues 26–36 including the switch I and switch I-preceding residues were pulled away from GppNHp. The WT, G12V, and Q61L structures were classified into state 1 judging from the loss of the Thr-35-γ-phosphate interaction (Figs. 1 and 2). Moreover, they lost the Gly-60-γ-phosphate direct hydrogen-bonding interaction. The side chains of Gln-61 in WT and G12V and of Leu-61 in Q61L oriented in an opposite direction away from the γ-phosphate compared to the corresponding residue in WT state 2 (Fig. 1).

3.2. Features of the state 1 structures of H-RasWT, G12V, and Q61L

The backbone structure of H-RasWT-GppNHp state 1 was compared with those of other state 1 conformers: H-RasT35S-GppNHp form 1 and 2 [6], H-RasG60A-GppNHp [7], and H-RasY32F-GppNHp [8]. It was superimposed very well on the backbone structures of T35S form 1 and G60A with rms deviations of 0.08 and 0.20 Å for 166 Cα atoms, respectively (Fig. 3A), but not those of Y32F and T35S form 2 with rms deviations of 1.17 Å and 1.18 Å for 164 and 155 Cα atoms, respectively (Fig. 3B). A marked difference existed in the conformation of residues 26–36, which was bent outward in WT state 1, T35S form 1, and G60A.

Intriguingly, the WT state 1 structure possessed two surface pockets, termed pocket 1 and 2, which were surrounded by the two switch regions and by the switch I-preceding residues 26-31 and GppNHp, respectively, as observed in T35S form 1 [6] (Fig. 4). Pocket 1 was composed of the residues 5–7, 12, 35–39, 54, 56, 59, 63–67, 70, 71 and 74, while pocket 2 was composed of the residues 18, 21, 22, 25, 27, 30–33, 146, 147, and 149. These pockets were unseen in the WT state 2 structure. The G12V and Q61L structures also possessed two pockets of similar shapes. However, there were some variations in the conformation of the residues comprising the margins of the pockets. The distance between Thr-35 and Glu-63 is longer in G12V and Q61L than in WT. Moreover, the side chain of Arg-149 of G12V but not WT and Q61L protruded at the edge of pocket 2. Furthermore, the bulky side chain of Val-12 of G12V protruded at the edge of pocket 1 near GppNHp. These structural differences of the pockets could be utilized for the structure-based drug design of Ras inhibitors selectively recognizing the activated mutants.

3.3. Structural basis for the lower GTPase activity of state 1 compared to state 2

Intrinsic GTP hydrolysis of Ras is known to depend on the location and orientation of the side chain of Gln-61 and of two water molecules (Wat-175 and Wat-189) activated by the side chain of Gln-61 to exert a nucleophilic attack on the γ-phosphate of GTP [4,20,21]. The bulky Val-12 side chain of the G12V mutant is thought to lower the GTPase activity through a steric interference over this catalytic process [20]. In the WT state 2 structure, Wat-175 and Wat-189 were located close enough to establish hydrogen bonds with the γ-phosphate (Fig. 2). Moreover, Wat-175 interacts

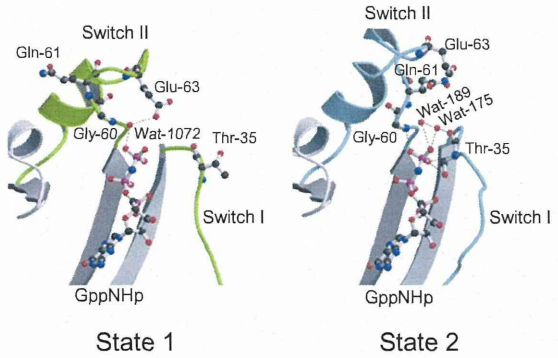

Fig. 2. Difference in the hydrogen-bonding patterns involving the γ-phosphate between WT state 1 and state 2. The two switch regions of state 1 (4EFL) and state 2 (5P21) are highlighted in *green* and *cyan*, respectively. Hydrogen bonds are indicated by *broken lines*. Thr-35, Gly-60, Gln-61, Glu-63, water molecules mediating the hydrogen bonds, and GppNHp are shown in the *ball-and-stick model*. For simplicity, magnesium ions and other water molecules are omitted.

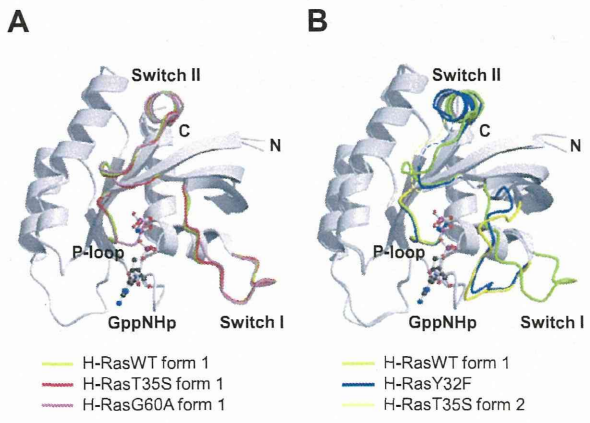

Fig. 3. Comparison of the overall structures of H-RasWT state 1 with other state 1 conformers. Superimposition of the backbone structures of the P-loop, switch I, and switch II among WT state1 (4EFL, *green*), T35S form 1 (3KKN, *red*), and G60A state 1 (1XCM, *violet*). The other regions are overlapped very well and shown in *gray*. GppNHp of WT state 1 is shown in the *ball-and-stick model*. Similar superimposition among WT state 1 (4EFL, *green*), Y32F state 1 (3K9N, *blue*), and T35S form 2 (3KKM, *yellow*). The backbone structures of the residues whose electron density is missing inY32F state 1 and T35S form 2 are shown by blue and yellow broken lines, respectively.

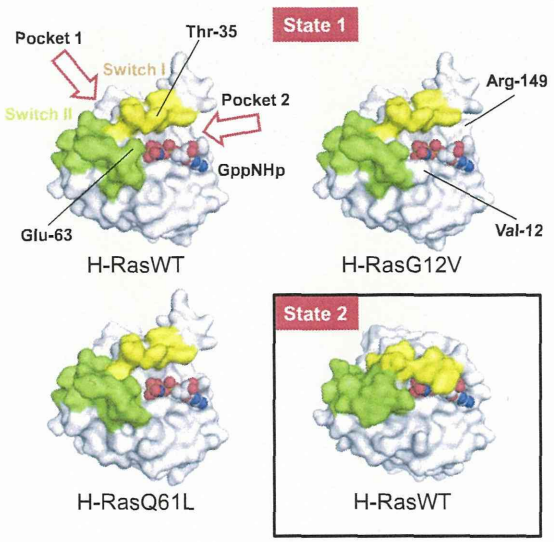

Fig. 4. Comparison of the surface pockets structures among WT state 1, G12V state 1, Q61L state 1, and WT state 2. Shown are the surface models of WT state 1 (4EFL), G12V state 1 (4EFM), Q61L state 1 (4EFN) and WT state 2 (5P21), which were generated by PyMOL (DeLano Scientific, LLC). Switch I and switch II are highlighted in *yellow* and *green*, respectively. GppNHp is shown by a *CPK model*. The two surface pockets of WT state 1 are shown by *red open arrows*.

directly with both Wat-189 and the main-chain carbonyl of Thr-35. By contrast, the WT state 1 structure possessed only one water molecule, Wat-1072, which was located close to the γ-phosphate and formed hydrogen bonds with both the γ-phosphate and the main-chain amide of Gly-60 but not with Thr-35. In addition, Wat-1072 formed a hydrogen bond with the side-chain carboxyl of Glu-63. Moreover, the side chain of Gln-61 in WT state 1 oriented away from the γ-phosphate, which was also observed in G12V, T35S form 1, Y32F, and G60A. It has recently been reported that H-Ras with higher state 2 populations exhibits accelerated GTPase activity, suggesting that state 1 possessed substantially lower GTPase activity compared state 2 [22]. Our results suggest that this reduction of the intrinsic GTPase activity may be accounted for by the gross alterations of the orientation of the Gln-61 side chain and the arrangement of the water molecules in state 1.

Acknowledgments

The synchrotron radiation experiments were performed at BL41XU in SPring-8 with the approval of Japan Synchrotron Radiation Research Institute (JASRI) (Proposal No. 2006A1786). We thank Drs. Kazuya Hasegawa, Nobutaka Shimizu, Seiki Baba, Nobuhiro Mizuno, and Masatomo Makino of JASRI/SPring-8 for data collection and helpful advices. This work was supported by Grants-in-Aid for Scientific Research from the Ministry of Health, Labour and Welfare and from the Ministry of Education, Science, Sports and Culture of Japan, and by a Grant from the National Institute of Biomedical Innovation.

Appendix A. Supplementary data

Supplementary data associated with this article can be found, in the online version, at http://dx.doi.org/10.1016/j.febslet.2012.04.058.

References

[1] Karnoub, A.E. and Weinberg, R.A. (2008) Ras oncogenes: split personalities. Nat. Rev. Mol. Cell. Biol. 9, 517–531.
[2] Vetter, I.R. and Wittinghofer, A. (2001) The guanine nucleotide-binding switch in three dimensions. Science 294, 1299–1304.
[3] Geyer, M., Schweins, T., Herrmann, C., Prisner, T., Wittinghofer, A. and Kalbitzer, H.R. (1996) Conformational transitions in p21^{ras} and in its complexes with the effector protein Raf-RBD and the GTPase activating protein GAP. Biochemistry 35, 10308–10320.
[4] Pai, E.F., Krengel, U., Petsko, G.A., Goody, R.S., Kabsch, W. and Wittinghofer, A. (1990) Refined crystal structure of the triphosphate conformation of H-ras p21 at 1.35 Å resolution:implications for the mechanism of GTP hydrolysis. EMBO J. 9, 2351–2359.
[5] Nassar, N., Horn, G., Herrmann, C., Scherer, A., McCormick, F. and Wittinghofer, A. (1995) The 2.2 Å crystal structure of the Ras-binding domain of the serine/threonine kinase c-Raf1 in complex with Rap1A and a GTP analogue. Nature 375, 554–560.
[6] Shima, F., Ijiri, Y., Muraoka, S., Liao, J., Ye, M., Araki, M., Matsumoto, K., Yamamoto, N., Sugimoto, T., Yoshikawa, Y., Kumasaka, T., Yamamoto, M., Tamura, A. and Kataoka, T. (2010) Structural basis for conformational dynamics of GTP-bound Ras protein. J. Biol. Chem. 285, 22696–22705.
[7] Ford, B., Skowronek, K., Boykevisch, S., Bar-Sagi, D. and Nassar, N. (2005) Structure of the G60A mutant of Ras: implications for the dominant negative effect. J. Biol. Chem. 280, 25697–25705.
[8] Buhrman, G., Holzapfel, G., Fetics, S. and Mattos, C. (2010) Allosteric modulation of Ras positions Q61 for a direct role in catalysis. Proc. Natl. Acad. Sci. USA 107, 4931–4936.
[9] Ye, M., Shima, F., Muraoka, S., Liao, J., Okamoto, H., Yamamoto, M., Tamura, A., Yagi, N., Ueki, T. and Kataoka, T. (2005) Crystal structure of M-Ras reveals a GTP-bound "off state conformation of Ras family small GTPases. J. Biol. Chem. 280, 31267–31275.
[10] Matsumoto, K., Shima, F., Muraoka, S., Araki, M., Hu, L., Ijiri, Y., Hirai, R., Liao, J., Yoshioka, T., Kumasaka, T., Yamamoto, M., Tamura, A. and Kataoka, T. (2011) Critical roles of interactions among switch I-preceding residues and between switch II and its neighboring α-helix in conformational dynamics of the GTP-bound Ras family small GTPases. J. Biol. Chem. 286, 15403–15412.
[11] Araki, M., Shima, F., Yoshikawa, Y., Muraoka, S., Ijiri, Y., Nagahara, Y., Shirono, T., Kataoka, T. and Tamura, A. (2011) Solution Structure of the State 1 Conformer of GTP-bound H-Ras Protein and Distinct Dynamic Properties between the State 1 and State 2 Conformers. J. Biol. Chem. 286, 39644–39653.
[12] Spoerner, M., Herrmann, C., Vetter, I.R., Kalbitzer, H.R. and Wittinghofer, A. (2001) Dynamic properties of the Ras switch I region and its importance for binding to effectors. Proc. Natl. Acad. Sci. USA 98, 4944–4949.
[13] Leslie, A.G.W. (1992) Recent changes to the MOSFLM package for processing film and image plate data. Joint CCP4 and ESF-EACBM Newsletter on Protein Crystallography, No. 26, Daresbury Laboratory, Warrington, UK.
[14] Collaborative Computational Project Number 4 (1994) The CCP4 suite: programs for protein crystallography. Acta Crystallogr. D50, 760–763.
[15] Murshudov, G.N., Vagin, A.A. and Dodson, E.J. (1997) Refinement of macromolecular structures by the maximum-likelihood method. Acta Crystallogr. D53, 240–255.
[16] Emsley, P. and Cowtan, K. (2004) Coot: model-building tools for molecular graphics. Acta Crystallogr. D60, 2126–2132.
[17] Bacon, D.J. and Anderson, W.F. (1988) A fast algorithm for rendering space-filling molecule pictures. J. Mol. Graph. 6, 219–220.
[18] Kraulis, P.J. (1991) MOLSCRIPT: a program to produce both detailed and schematic plots of protein structures. J. Appl. Crystallogr. 24, 946–950.
[19] Spoerner, M., Wittinghofer, A. and Kalbitzer, H.R. (2004) Perturbation of the conformational equilibria in Ras by selective mutations as studied by ^{31}P NMR spectroscopy. FEBS Lett. 578, 305–310.
[20] Krengel, U., Schlichting, I., Scherer, A., Schumann, R., Freeh, M., John, J., Kabsch, W., Pai, E.F. and Wittinghofer, A. (1990) Three-dimensional structures of H-ras p21 mutants: molecular basis for their inability to function as signal switch molecules. Cell 62, 539–548.
[21] Scheidig, A.J., Burmester, C. and Goody, R.S. (1999) The pre-hydrolysis state of p21^{ras} in complex with GTP: new insights into the role of water molecules in the GTP hydrolysis reaction of ras-like proteins. Structure 7, 1311–1324.
[22] Spoerner, M., Hozsa, C., Poetzl, J.A., Reiss, K., Ganser, P., Geyer, M. and Kalbitzer, H.R. (2010) Conformational states of human rat sarcoma (Ras) protein complexed with its natural ligand GTP and their role for effector interaction and GTP hydrolysis. J. Biol. Chem. 285, 39768–39778.